

[19002]

照射誘起アモルファス化へのFeイオンビーム影響 Effect of iron beam on radiation-induced amorphization

叶野翔^{A)}, 楊会龍^{A)}, John McGrady^{A)}, 安堂正己^{B)}, 濱口大^{B)}, 谷川博康^{B)}, 阿部弘亨^{A)}
Sho Kano^{A)}, Huilong Yang^{A)}, John McGrady^{A)}, Masami Ando^{B)},
Dai Hamaguchi^{B)}, Hiroyasu Tanigawa^{B)}, Hiroaki Abe^{A)}

^{A)} Nuclear Professional School, School of Engineering, The University of Tokyo

^{B)} National Institutes for Quantum and Radiological Science and Technology (QST),
Research and Development Center

Abstract

The mechanical properties of reduced activation ferritic/martensitic steels (RAFMs) such as creep, thermal aging, and irradiation resistance are improved by the formation of MX and $M_{23}C_6$ particles, these particles are however unstable under irradiation. The purpose of the present study is to clarify the details of the radiation-induced amorphization (RIA) of $M_{23}C_6$ in F82H steels. The instability behavior of $M_{23}C_6$ under a wide range of irradiation temperatures from R.T. to 773 K and various ion beam energies (2.8, 3.7, 6.4 and 10.5 MeV) was investigated. Two types of materials, F82H and its model alloy (F8), were utilized in this study. TEM observation and selected area electron diffraction analysis before and after irradiation were conducted to evaluate the occurrence of RIA. In the case of the iron irradiation at the temperature below 598 K, a bilayer contrast of the particle, consisting of an amorphous-rim phase and inner crystalline core, was observed. Similar particle survived in the irradiated F82H at the temperature of 623 K, the RIA was not observed in the F8 specimen. Consequently, the critical temperature of RIA was estimated as 623–673 K. Since the melting temperature (T_m) of $M_{23}C_6$ is approximately 2173 K, the critical temperature corresponds to $\sim 0.29 T_m$.

Keyword: F82H steel, $M_{23}C_6$, ion irradiation, amorphization

1. Introduction

Reduced activation ferritic/martensitic steels (RAFMs) are considered as the main candidate materials for structural applications in the fusion DEMO reactor blanket. Lots of efforts have been made on the development and characterization of these materials, such as F82H in Japan^[1] and Eurofer97 in EU^[2]. Fine particles such as $M_{23}C_6$ and MX are controlling factors of mechanical properties of these materials, extensive studies on the evaluation of these materials have been reported^[3-10].

In our previous studies, the instability of the fine particles in F82H steel was evaluated via in-situ observations under high voltage electron microscopy (HVEM) and ion irradiation at elevated temperatures^[11-14]. The feature of instability behavior of MX and its kinetics were proposed based on the experimental observation. On the other hand, the instability of $M_{23}C_6$ particles in F82H steel under HVEM irradiation exhibited a strong dependence upon irradiation temperature and damage level. Previously, the amorphization of $M_{23}C_6$ under neutron and ion irradiations at the temperature of < 573 K have been investigated. Tanigawa et.al. reported that the radiation induced amorphization (RIA) occurred in both of $M_{23}C_6$ and laves phases^[9], where the laves phase is formed by thermal aging of 1.08×10^8 s at 873 K, and the ion irradiation was performed at 573 K up to 10 dpa. This study also pointed out that the RIA of the laves phase is more likely to be relative to $M_{23}C_6$. Sencer et.al. reported the phase stability of fine particle in a modified 9Cr–1Mo

ferritic/martensitic steel irradiated by mixed proton and spallation neutron at temperatures below 333 K with a dose of 0.5–9.6 dpa^[15], and the results showed that the $M_{23}C_6$ was completely amorphized at the damage level of 0.5 dpa.

Regarding the instability of the $M_{23}C_6$ particle, both the critical dose level and temperature are important indicators. Compared with the irradiation damage of the F82H suffered under a fusion reactor environment, which can hypothetically reach up to ~ 100 dpa, the critical dose level required for RIA (D_c) is thus presumed to be relatively low. On the other hand, although the critical temperature for RIA (T_c) is estimated at ~ 573 K from the previous study, in a strict sense, it requires a systematic survey covering a much wider temperature range, rather than the estimation at the irradiation temperature of 573 K. The systematic investigation on RIA of $M_{23}C_6$ has been scarcely investigated, and the understanding of this behavior is not yet fully clarified. Therefore, the purpose of the present study is to clarify the critical temperature for the amorphization of $M_{23}C_6$ in F82H steel, the morphological change of $M_{23}C_6$ particles under the ion accelerator irradiations at various temperature was investigated.

2. Experimental procedures

Two types of specimens, RAFMs and its model alloy which will be named as F82H and F8 hereafter, were used in this study. The chemical compositions of F82H is Fe-0.1C-7.88Cr-1.78W-0.19V-0.09Ta-0.45Mn-0.022Al-

[19002]

0.0010-0.001N. The heat treatment condition for normalizing and tempering of F82H was 1313 K for 2.4 ks and 1023 K for 3.6 ks, respectively. Detailed information on the thermal history of this specimen can be seen elsewhere [16]. On the other hand, the chemical composition of the F8 specimen is simplified in comparison with F82H, only 8.0%-Cr and 0.1%-C are included as the alloying elements in iron. The tempering process at 1023 K for 3.6 ks with air cooling (A.C.) was performed after the solution heat treatment (1523 K for 86.4 ks with water quenching (W.Q.)) without the normalizing process. The $M_{23}C_6$ particles are dispersed into the lath-martensite structure, and the effect of solid solution elements into the matrix and dissolution W into the particle is negligible in this specimen.

Specimens with a size of $1 \times 3 \times 5 \text{ mm}^3$ were prepared for the ion irradiation. They were firstly cut from the bulk specimen, and the surface was subsequently mechanically polished by the emery papers, and they were further mirror-finished by polishing. After that, the deformed layer by mechanical polishing was removed by electrochemically etching in a solution (8%-perchloric acid in acetic acid).

Three type of accelerators, which are respectively HIT at The University of Tokyo, DuET at Kyoto University and TIARA at National Institutes for Quantum and Radiological Science and Technology, were used for the irradiation in this study. The iron irradiations (Fe^{n+}) with the energy of 2.8, 3.7, 6.4 and 10.5 MeV were selected. A wide range of irradiation temperatures including 289, 373, 450, 473, 573, 598, 623, 673 and 773 K were conducted to assess the presence and absence of RIA of $M_{23}C_6$ under each irradiation condition. The depth profiles of irradiation damage was evaluated with SRIM calculation code [17, 18]. The damage rate is determined based on the average Fe-beam flux and the SRIM displacement calculation with the Kinchin-Pease model. The threshold displacement energy for Fe was set as 40 eV [17, 18] in this calculation. The depth at the damage peak of 2.8, 3.7, 6.4 and 10.5 MeV irradiations are respectively ~ 0.8 , ~ 1.0 , ~ 1.4 and $\sim 1.8 \mu\text{m}$, with the corresponding irradiation rate of 8.2, 7.4, 5.1, and 11.0×10^{-4} dpa/s, respectively. In addition, the temperature of the specimen during irradiation was monitored and recorded by a thermocouple located at the vicinity of specimen. The temperature was measured within the fluctuation of ± 5 K for all the irradiations. Obvious beam heating was not measured in this study.

After irradiation, cross-sectional transmission electron microscopy (TEM) observation was conducted to investigate microstructural changes due to the irradiation. A standard lift-out method using the focused ion beam (FIB) technique was applied to prepare the thin TEM specimens. The acceleration voltage of Ga ions was set to 40 kV, and a W-deposit layer was applied to protect the thin foil from the irradiation damage induced by Ga-ion. Low energy Ar ion milling was further performed before

TEM observation to eliminate the artificial defects induced during FIB processing. Two steps of low-energy Ar ion milling process was performed. First step was performed at a working voltage of 1.0-kV until the black dot contrast in the unirradiated region substrate disappeared. As a second step, a lower acceleration voltage of Ar ion milling at a working voltage of 0.3 kV was conducted to eliminate the amorphous layer formed by the 1.0 kV-Ar ion milling. The beam currents of 1.0- and 0.3-kV Ar milling were ~ 13 and $2 \mu\text{A}$, respectively.

TEM observation and scanning transmission electron microscopy-energy dispersive X-ray spectrometry (STEM-EDS) mapping were conducted working at 200-keV. Bright field (BF), dark field (DF) and high resolution TEM (HRTEM) observations with the selective area electron diffraction (SAED) analysis were utilized to evaluate the morphological change of the particles. The thickness of the specimen was estimated by the thickness fringe technique in order to determine the number density of particles. The average size and number density of particles were determined from ~ 50 particles after confirming their chemical compositions by STEM-EDS analysis, because the Cr-rich $M_{23}C_6$ and Ta- and V-rich MX are co-existed in the F82H steel. For STEM-EDS mapping, the electron probe size and scanning step were set as 0.2 and 4.4 nm, respectively. The characteristic X-rays of Fe- K_{α} , Cr- K_{α} , W- M_{α} , V- K_{α} , and Ta- M_{α} were used in this study.

3. Results and Discussion

3.2 Feature $M_{23}C_6$ particle in unirradiated specimens

From the TEM observation of unirradiated F82H and F8 specimen, the spherical and orbital shape of the particles were observed in both specimens. The average size of the particles in F82H and F8 specimens were estimated as 47.2 and 68.8 nm, and the number densities were 2.31 and $4.49 \times 10^{13} \text{ cm}^{-3}$, respectively. The volume of $M_{23}C_6$ particles in the F8 specimen which is the integral value from the average size and number density is higher than that in F82H. The reason behind this behavior is considered as follows: the carbon concentration of these specimens is approximately 0.1 wt. %, the carbon source for the formation of $M_{23}C_6$ particle in F82H is decreased because some of the carbon atoms are consumed to form the MX type carbides.

The BF, HRTEM images and SAED pattern of F82H specimen irradiated to 20 dpa by 10.5 MeV- Fe^{3+} at 598 K are shown in **Figure 1**. The spherical and/or orbital shape of particles which consisted of multiple changes in contrast were observed in the BF micrograph. The diffraction spots from the particle were further observed from the SAED pattern. The crystal structure of particle was observed in the HRTEM image which is corresponded to the lower contrast region of BF micrograph. On the other hands, the crystallinity of the region of surrounding

[19002]

particle was not identical by the HRTEM micrograph, which is indicated that the amorphous phase was existed in this region. Therefore, the $M_{23}C_6$ particle surrounded by an amorphous rim was formed by the irradiation, such kind of bilayer structure particle infers the occurrence of RIA in $M_{23}C_6$.

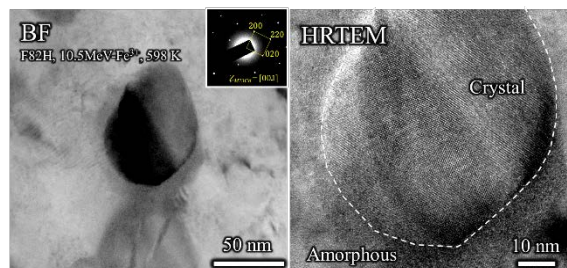


Figure 1. The morphology of $M_{23}C_6$ in F82H irradiated to 20 dpa by 10.5 MeV- Fe^{3+} at 598 K. The images were exposed from the $Z_{M_{23}C_6} = 001$ of the particle.

The bilayer-contrast particle was observed in specimen of F82H irradiated to 20 dpa by 10.5 MeV- Fe^{3+} at 623 K, whose morphology is similar to the specimen irradiated at 598 K as shown in **Figure 1**. The co-existence of diffraction spots from Fe-matrix, $M_{23}C_6$ and halo-ring can be seen from the SAED image. DF micrograph exposed from the halo-ring was taken to emphasize the amorphous region of the particle in the BF image, indicating that the RIA of $M_{23}C_6$ occurred under irradiation at 623 K in the F82H specimen. On the other hand, the bilayer-contrast of particle was not observed in the specimen of F8 irradiated to 20 dpa by 10.5 MeV- Fe^{3+} at 623 K, and halo-ring was not observed neither by SAED. Therefore, it was found that the crystalline $M_{23}C_6$ particle with a lattice constant ~ 1.06 nm survived after irradiation at 623 K up to 20 dpa in the F8 specimen. In addition, the halo-ring appeared in SAED images of irradiated F82H subjected to 3.7 MeV-1.0 dpa at 298 K and 2.8 MeV-10 dpa at 573 K, as well as the amorphous- and crystal-region of $M_{23}C_6$ were clearly co-existed, which is similar with the feature of RIA in 10.5 MeV irradiated specimens. More results about the high-temperature irradiation in $M_{23}C_6$ particles has been previously reported elsewhere [13]. Therefore, the critical temperature for RIA of $M_{23}C_6$ in F82H was roughly estimated as >623 K, which is 50 K higher compared with the previous results [9,15]. Regarding the variation in the critical temperature of RIA between the F82H and F8 specimen, this mechanism is still unclear, but the chemical composition of the particle such as Cr, Fe and W may exert an influence to the RIA.

Figure 2 shows the phase diagram regarding the RIA of $M_{23}C_6$ particle in the F82H specimen, which displays the relationship between the displacement damage and irradiation temperature under various ion energy

irradiation conditions. The occurrence of RIA is determined by whether a halo-ring is present or absent in SAED, and a clear contrast can be achieved or not in the DF imaging by exposing the halo-ring. The “○” mark in **Figure 2** means a higher contrast of particle was confirmed in the DF image from the halo-ring, and the condition that all $M_{23}C_6$ particles with intact crystallinity after irradiation is indicated as “×”. The irradiation was conducted using 2.8, 3.7, 6.4 and 10.5 MeV Fe-ions at temperatures from RT to 773 K, and the microstructure observation was performed respectively at 0.4, 0.5, 0.7 and 1.0 μm away from the irradiated top surface, in which the damage rate was corresponded to $3.9\text{-}1.8 \times 10^{-4}$ dpa/s. As a result, the critical dose and temperature of RIA in $M_{23}C_6$ could be respectively estimated as ~ 1.0 dpa and ~ 623 K from this study. Since the melting temperature (T_m) of $M_{23}C_6$ is approximately 2173 K, the critical temperature corresponds to $\sim 0.29 T_m$.

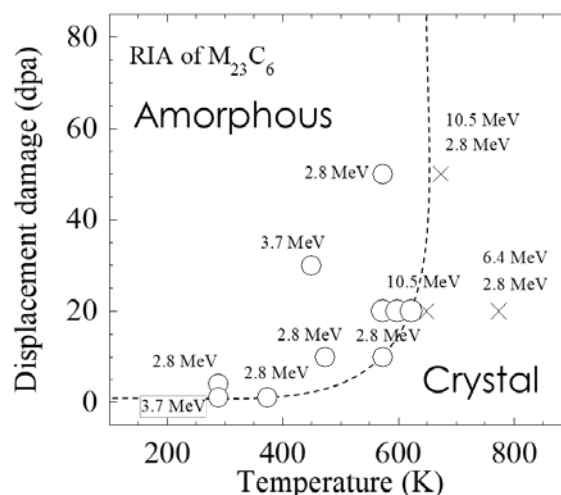


Figure 2. The phase diagram of RIA of $M_{23}C_6$ particle under several ion irradiation conditions. The “○” mark means a higher contrast of particle was gained in DF image from halo-ring, and the condition that all $M_{23}C_6$ particle in the irradiation region had crystallinity is indicated as “×”.

With regard to the effect of ion energy on the RIA of $M_{23}C_6$ particles in F82H, it is considered to be minimal if there is any. Previously, Abe et al. reported the effects of damage rate and irradiation beam energy on the RIA of graphite with in-situ observation under ion and electron irradiations [23], in which, the irradiations with 200 keV- He^+ , 300 keV- C^+ , 300 keV- Ne^+ , 600 keV- Ar^{2+} , and 600 keV- Xe^{2+} were performed with accelerating voltage from 200 to 300 kV and ion fluxes from 10^{17} to 10^{18} ions/ m^2 s. As a result, the critical temperature of RIA increased with increasing accelerating ion energy and saturated at ion energy above ~ 300 keV. It is supposed that the RIA

[19002]

behavior is dependent on the material properties, and the T_c/T_m of graphite material is estimated as $\sim 0.21 T_m$. Despite the direct comparison with the RIA behavior of $M_{23}C_6$ might be difficult, it is however considered that the effect of beam energy will be negligible because Fe^{n+} beams with the energy at the order of $\sim MeV$ are utilized in this study, which is much higher than that is the RIA of graphite material. Data on the effect of damage rate for RIA is still limited in the case of $M_{23}C_6$, as such further evaluation is required to clarify the detail. The evaluation of the effect of damage rate is ongoing in order to elucidate the mechanism of RIA under irradiation, and the related findings will be reported elsewhere.

4. Conclusions

As one of the unstable behaviors of $M_{23}C_6$ particle in the F82H steel under irradiation, the RIA of $M_{23}C_6$ particle in F82H and its model alloy (F8) was systematically investigated by ion accelerator irradiations under various energies at temperatures from R.T. to 773 K. After irradiation, detailed TEM observation was conducted. The main results of this study are summarized as follows:

(1) The spherical and orbital shape of $M_{23}C_6$ particles dispersed into the lath-martensite matrix were observed in both specimens. The average size of these particles in F82H and F8 specimens were estimated as 47.2 and 68.8 nm, and the number densities were 2.31 and $4.49 \times 10^{13} \text{ cm}^{-3}$, respectively.

(2) A bilayer contrast of $M_{23}C_6$ particle, consisting of an amorphous rim and inner crystalline core, was observed after irradiation. From the SAED analysis with DF micrograph observation, the critical temperature for RIA of $M_{23}C_6$ was estimated as 623-673 K, which corresponds to $0.29 T_m$.

References

- [1] [1] A. Hishinuma, A. Kohyama, R.L. Klueh, D.S. Gelles, W. Dietz, K. Ehrlich, Current status and future R&D for reduced-activation ferritic/martensitic steels, *J. Nucl. Mater.*, 258-263 (1998) 193-204, [https://doi.org/10.1016/S0022-3115\(98\)00395-X](https://doi.org/10.1016/S0022-3115(98)00395-X).
- [2] D. Dulieu, K.W. Tupholme, G.J. Butterworth, Development of low-activation martensitic stainless steels, *J. Nucl. Mater.*, 141-143 (1986) 1097-1101, [https://doi.org/10.1016/0022-3115\(86\)90148-0](https://doi.org/10.1016/0022-3115(86)90148-0).
- [3] H. Tanigawa, E. Gaganidze, T. Hirose, M. Ando, S.J. Zinkle, R. Lindau, E. Diegele, Development of benchmark reduced activation ferritic/martensitic steels for fusion, *Nucl. Fusion*, 57 (2017) 092004 (13pp), <https://doi.org/10.1088/1741-4326/57/9/092004>.
- [4] L. Tan, Y. Katoh, A.-A.F. Tavassoli, J. Henry, M. Rieth, H. Sakasegawa, H. Tanigawa, Q. Huang, Recent status and improvement of reduced-activation ferritic-martensitic steels for high-temperature service, *J. Nucl. Mater.*, 479 (2016) 515-523, <https://doi.org/10.1016/j.jnucmat.2016.07.054>.
- [5] A.-A.F. Tavassoli, Present limits and improvements of structural materials for fusion reactors – a review, *J. Nucl. Mater.*, 302 (2002) 73-88, [https://doi.org/10.1016/S0022-3115\(02\)00794-8](https://doi.org/10.1016/S0022-3115(02)00794-8).
- [6] M.A. Sokolov, H. Tanigawa, G.R. Odette, K. Shiba, R.L. Klueh, Fracture toughness and Charpy impact properties of several RAFMS before and after irradiation in HFIR, *J. Nucl. Mater.*, 367-370 (2007) 68-73, <https://doi.org/10.1016/j.jnucmat.2007.03.165>.
- [7] H. Tanigawa, K. Shiba, A. Möslang, R.E. Stoller, R.L. Rindau, M.A. Sokolov, G.R. Odette, R.J. Kurtz, S. Jitsukawa, Status and key issues of reduced activation ferritic/martensitic steels as the structural material for a DEMO blanket, *J. Nucl. Mater.*, 417 (2011) 9-15, <https://doi.org/10.1016/j.jnucmat.2011.05.023>.
- [8] H. Tanigawa, T. Hirose, K. Shiba, R. KaSAEDa, E. Wakai, H. Serizawa, Y. Kawahito, S. Jitsukawa, A. Kimura, Y. Kohno, A. Kohyama, S. Katayama, H. Mori, K. Nishimoto, R.L. Klueh, M.A. Sokolov, R.E. Stoller, S.J. Zinkle, Technical issues of reduced activation ferritic/martensitic steels for fabrication of ITER test blanket modules, *Fusion Eng. & Des.*, 83 (2008) 1471-1476, <https://doi.org/10.1016/j.fusengdes.2008.07.024>.
- [9] H. Tanigawa, H. Sakasegawa, H. Ogiwara, H. Kishimoto and A. Kohyama, Radiation induced phase instability of precipitates in reduced-activation ferritic/martensitic steels, *J. Nucl. Mater.*, 367-370 (2007) 132-136, <https://doi.org/10.1016/j.jnucmat.2007.03.155>.
- [10] X. Jia, Y. Dai, Microstructure in martensitic steels T91 and F82H after irradiation in SINQ Target-3, *J. Nucl. Mater.*, 318 (2003) 207-214, [https://doi.org/10.1016/S0022-3115\(03\)00101-6](https://doi.org/10.1016/S0022-3115(03)00101-6).
- [11] H. Abe, T. Ishizaki, F. Li, S. Kano, Y. Li, Y. Satoh, T. Nagase and H. Yasuda, New approach to in situ observation experiments under irradiation in high voltage electron microscopes, *Mater. Trans.*, 55 (2014) 423-427, <https://doi.org/10.2320/matertrans.MD201315>.
- [12] H. Abe, T. Ishizaki, S. Kano, F. Li, Y. Satoh, H. Tanigawa, D. Hamaguchi, T. Nagase, H. Yasuda, Mechanism of instability of carbides in Fe-TaC alloy under high energy electron irradiation at 673 K, *J. Nucl. Mater.*, 455 (2014) 695-699, <https://doi.org/10.1016/j.jnucmat.2014.08.032>.
- [13] S. Kano, H. Yang, J. Shen, Z. Zhao, M. John, D. Hamaguchi, M. Ando, H. Tanigawa, H. Abe, Investigation of instability of $M_{23}C_6$ particles in F82H steel under electron and ion irradiation conditions, *J. Nucl. Mater.*, 502 (2018) 263-269, <https://doi.org/10.1016/j.jnucmat.2018.02.004>.
- [14] S. Kano, H.L. Yang, J.J. Shen, Z. Zhao, J. McGrady, D. Hamaguchi, M. Ando, H. Tanigawa and H. Abe, Instability of MX and $M_{23}C_6$ type precipitates in F82H steels under 2.8 MeV Fe^{2+} irradiation at 673 K, *Nucl. Mater. & Energy*, 17 (2018) 56-61, <https://doi.org/10.1016/j.nme.2018.08.001>.
- [15] B.H. Sencer, F.A. Garner, D.S. Gelles, G.M. Bond, S.A. Maloy, Microstructural evolution in modified 9Cr-1Mo ferritic/martensitic steel irradiated with mixed high-energy proton and neutron spectra at low temperatures, *J. Nucl. Mater.*, 307-311 (2002) 266-271, [https://doi.org/10.1016/S0022-3115\(02\)01198-4](https://doi.org/10.1016/S0022-3115(02)01198-4).
- [16] H. Sakasegawa, H. Tanigawa, S. Kano, H. Abe, Material properties of the F82H melted in an electric arc furnace, *Fusion Eng. & Des.*, 98-99 (2015) 2068-2071, <https://doi.org/10.1016/j.fusengdes.2015.06.103>.
- [17] J.F. Ziegler, J.M. Manoyan, The stopping of ions in compounds, *Nucl. Inst. & Methods*, B35 (1988) 215-228, [https://doi.org/10.1016/0168-583X\(88\)90273-X](https://doi.org/10.1016/0168-583X(88)90273-X).
- [18] K. Nordlund, J. Wallenius, L. Malerba, Molecular dynamics simulations of threshold displacement energies in Fe, *Nucl.*

[19002]

- Instr. & Meth. B, 246 (2006) 322-332,
<https://doi.org/10.1016/j.nimb.2006.01.003>.
- [19] S. Kano, H. Yang, R. Suzue, Y. Matsukawa, Y. Satoh, H. Sakasegawa, H. Tanigawa, H. Abe, Precipitation of carbides in F82H steels and its impact on mechanical strength, Nucl. Mater. & Energy, 9 (2016) 331-337,
<https://doi.org/10.1016/j.nme.2016.09.017>.
- [20] K. Fukumoto, T. Sakaguchi, K. Inoue, T. Itoh, H. Sakasegawa, H. Tanigawa, Dependence of precipitate formation on normalizing temperature and its impact on the heat treatment of F82H-BA07 Steel, J. Nucl. Mater., 442 (2013) S28-S32,
<https://doi.org/10.1016/j.jnucmat.2013.02.065>.
- [21] A.L. Bowman, G.P. Arnold, E.K. Storms, N.G. Nereson, The crystal structure of Cr₂₃C₆, Acta Cryst. (1972). B28, 3102-3103,
<https://doi.org/10.1107/S0567740872007526>.
- [22] C.M. Fang, M.A. van Huis, M.H.F. Sluiter, Formation, structure and magnetism of the γ -(Fe,M)₂₃C₆ (M = Cr, Ni) phases: A first-principles study, Acta Mater., 103 (2016) 273-279,
<https://doi.org/10.1016/j.actamat.2015.08.078>.
- [23] Hiroaki Abe, Hiroshi Naramoto, Akihiro Iwase, Chiken Kinoshita, Effect of damage cascades on the irradiation-induced amorphization in graphite, Nucl. Instr. & Meth. in Phys. Res. B, 127 (1997) 681-684,
[https://doi.org/10.1016/S0168-583X\(96\)01155-X](https://doi.org/10.1016/S0168-583X(96)01155-X).